applied sciences

MDPI

Article

Feasibility of a Drug-Releasing Radiofrequency Ablation System in a Porcine Liver Model

Young Chul Cho [1,†], Ki Baek Lee [2,†], Su Jung Ham [1], Jin Hwa Jung [3], Yubeen Park [2], Dong-Sung Won [2], Kyung Won Kim [1,*] and Jung-Hoon Park [2,*]

1 Department of Radiology and Research Institute of Radiology, Asan Medical Center, University of Ulsan College of Medicine, Seoul 05505, Korea; youngchulcho@amc.seoul.kr (Y.C.C.); mission02@amc.seoul.kr (S.J.H.)
2 Biomedical Engineering Research Center, Asan Institute for Life Sciences, Asan Medical Center, Seoul 05505, Korea; beall34@amc.seoul.kr (K.B.L.); ybeen9733@amc.seoul.kr (Y.P.); ehdtjd3004@amc.seoul.kr (D.-S.W.)
3 Convergence Medicine Research Center, Asan Institute for Life Sciences, Asan Medical Center, Seoul 05505, Korea; morality67@amc.seoul.kr
* Correspondence: kyungwon_kim@amc.seoul.kr (K.W.K.); jhparkz@amc.seoul.kr (J.-H.P.); Tel.: +82-2-3010-4377 (K.W.K.); +82-2-3010-4123 (J.-H.P.)
† Y.C.C. and K.B.L. contributed equally to this work and are the co-first authors.

Abstract: The objective of this study was to investigate the feasibility of a newly developed anticancer drug-releasing radiofrequency ablation (RFA) system in a porcine liver model. A 15-gauge drug-releasing cooled wet electrode (DRCWE) was newly developed to improve the RFA efficacy for creating a large ablation as well as for simultaneously delivering an anticancer drug to the tumor margin. Nine ablations in three pigs were performed by the DRCWE. The sectioned liver specimens were evaluated by measuring the ablation zone by a positron emission tomography/magnetic resonance imaging examination to investigate whether ^{18}F-fluorodeoxyglucose was exactly diffused. Volumes of the ablation zones released drug injection volumes, circularity, retention rate defined as the ratio between an estimated and injection dose, and the standard uptake value were assessed. The drug-releasing RFA was technically successful without procedural-related complications. During the procedure, the color changes of the ablated zones of the liver were observed in all specimens. The mean drug injection volume was higher than the ablated volumes (17.21 ± 2.85 vs. 15.22 ± 2.30 cm^3) and the circularity was 0.72 ± 0.08. Moreover, the retention rate was $72.89\% \pm 4.22\%$ and the mean standard uptake value was 0.44 ± 0.05. The drug-releasing RFA system was feasible not only for local ablation but also for the delivery of anticancer drugs. The results of this study indicate that this novel strategy of localized RFA with a drug delivery system could be a promising option for the prevention of local recurrence rates.

Keywords: drug-releasing radiofrequency ablation; anticancer drug-releasing cooled wet electrode; local recurrence rate

Citation: Cho, Y.C.; Lee, K.B.; Ham, S.J.; Jung, J.H.; Park, Y.; Won, D.-S.; Kim, K.W.; Park, J.-H. Feasibility of a Drug-Releasing Radiofrequency Ablation System in a Porcine Liver Model. *Appl. Sci.* **2021**, *11*, 8301. https://doi.org/10.3390/app11188301

Academic Editor: Alfonso Zambon

Received: 25 August 2021
Accepted: 6 September 2021
Published: 7 September 2021

1. Introduction

Image-guided radiofrequency ablation (RFA) has been widely performed as a minimally invasive therapeutic option utilizing thermal energy for early-stage hepatocellular carcinoma (HCC) in patients who are not surgical candidates [1,2]. Moreover, RFA is being increasingly used in various clinical practices with advances in probe types and ablation techniques for primary and secondary liver malignancies instead of hepatic resection [2–4]. RFA has a limitation that needs to be addressed priorly, including a higher local recurrence rate than that of surgical resection, although RFA is a major technique for liver tumor treatment. The main cause of the higher local recurrence rate associated with RFA is inadequate volumes of tumor ablation [4–6]. The local recurrence rate is still high although combination therapy with other modalities, such as transcatheter arterial

chemoembolization, saline injection, and percutaneous ethanol injection, can be helpful to improve clinical outcomes [6–12].

Several RFA electrodes have been developed to improve this weak point and expand the ablation range, e.g., the RFA with new types of electrodes (e.g., the multitier expandable needle electrodes with saline infusion and perfusion electrodes) and multiple electrodes for different applications of RF energy (e.g., the multipolar and the switching monopolar modes) [13–17]. Similarly, this study evaluated a new drug-releasing RFA system, which can deliver an anticancer drug to achieve sufficient treatment around the targeted tumor to increase clinical outcomes with a low recurrence rate. This preliminary study started with the hypothesis that anticancer drugs used in combination with RFA could lead to therapeutic outcome improvement and recurrence rate decrease for the local treatment of primary HCC (Figure 1). Therefore, this study aims to investigate the feasibility of a newly developed anticancer drug-releasing RFA system in a porcine liver model.

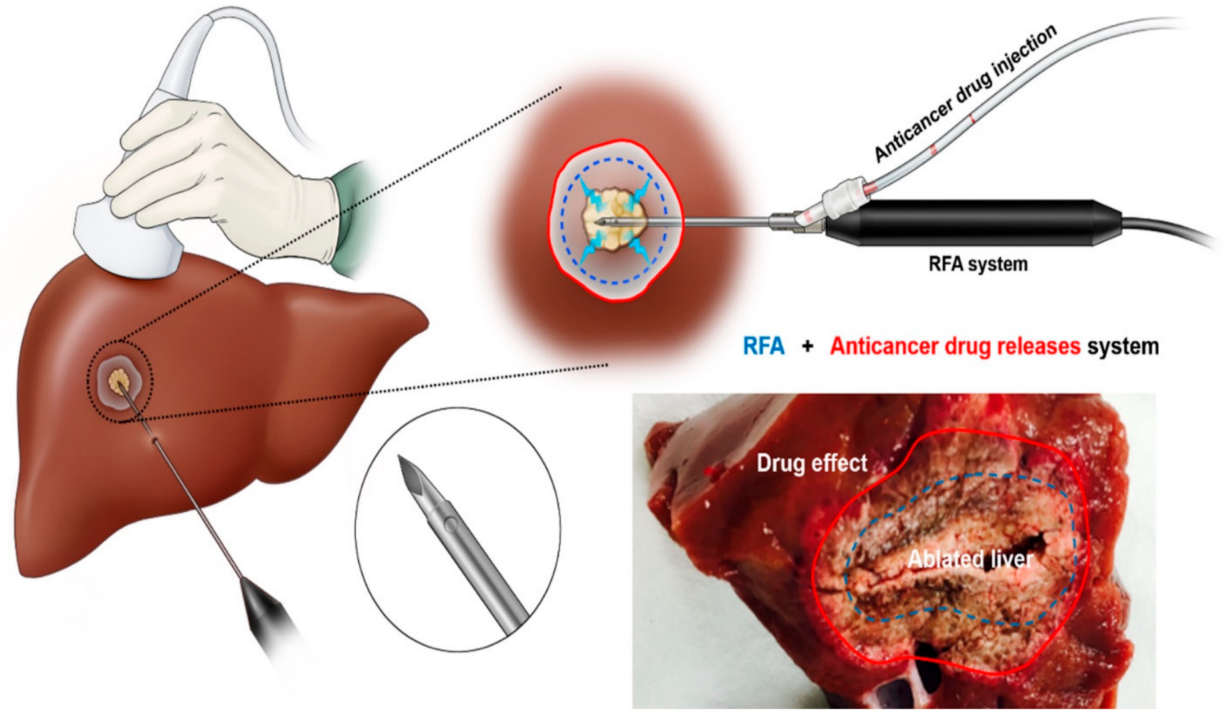

Figure 1. Schematic illustration of a radiofrequency ablation (RFA) system. The drug-releasing RFA system provides local ablation therapy with the delivery of anticancer drugs.

2. Materials and Methods

2.1. Drug-Releasing RFA System

A multichannel RFA system (M-3004; RF Medical Co., Seoul, Korea) was used in this study. It provided the automatic switching of RF energy among the three electrodes according to impedance changes in either monopolar or bipolar modes. An RF generator had a maximum power of 200 W at a frequency of 400 kHz consisting of each separate channel for the three electrodes (Figure 2a).

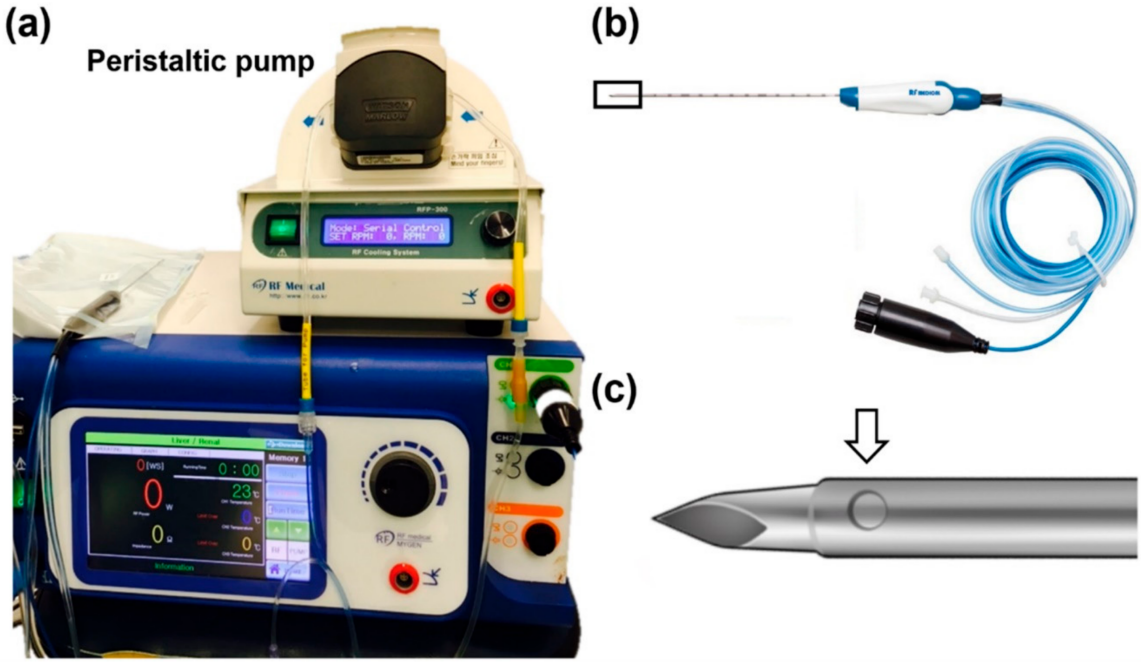

Figure 2. The radiofrequency ablation (RFA) system configuration. (**a**) A three-channel radiofrequency ablation system, which can allow the use of multiple electrodes in either monopolar or bipolar modes. (**b**) An internally cooled wet electrode with a 2-cm active tip. (**c**) The magnified image of the DRCWE tip with a side hole (white arrow).

A 15-gauge drug-releasing cooled wet electrode (DRCWE) was newly developed for this study. The DRCWE consisted of a 15-gauge internally cooled electrode with 2-cm active tips and two small side holes (diameter = 0.03 mm), allowing the simultaneous delivery of anticancer drugs to the tumor margin as well as creating a large ablation (Figure 2b,c). Internal cooling was ensured by using approximately 99% of the chilled isotonic saline (0.9%) circulated inside the electrode at rates of 0.8 mL/min. Moreover, the remaining 1% was utilized for saline infusion into the surrounding tissue at a rate of 1.2 mL/min. A peristaltic pump (RFP-300; Cardiva Medical Inc., Santa Clara, CA, USA) was used to infuse normal saline at 5–10 °C into the lumen of the electrode to maintain a tip temperature of 10–25 °C.

2.2. In Vivo Drug-Releasing RFA Procedure

This study was approved by the local Institutional Animal Care and Use Committee and performed following the guidelines of the National Institutes of Health for the humane handling of animals. Nine RFA zones (three ablations per pig) were performed by one radiologist with >10 years of experience under intraoperative ultrasonographic guidance to minimize potential variations in the procedural outcomes. An RF electrode was placed in the liver under real-time ultrasound guidance away from intrahepatic vessels, interlobar fissure, or the liver capsule so that the RFA zone would not be influenced by these structures. The distance between the center of each ablation zone was kept at least 5 cm apart to avoid ablation zone attachment.

The pigs were anesthetized using an intramuscular injection of tiletamine–zolazepam mixture (7.5 mg/kg; Zoletil 50; Virbac Korea Co., Seoul, Korea) and xylazine hydrochloride (2 mg/kg; Rompun; Bayer Korea Ltd., Ansan, Korea). Moreover, anesthesia was maintained with inhaled isoflurane of 1.5% in 100% oxygen (Forane Solution; Choongwae Pharma Co., Seoul, Korea) by endotracheal intubation. Cardiac status with electrocardiography, including heart rate, blood pressure, and oxygen saturation was monitored throughout the procedure. The pigs were placed in the supine position and vital signs were monitored. Two ground pads were placed on both shaved thighs connected in parallel to the RF generator. The liver was exposed by laparotomy after the epigastric

area was sterilized. Moreover, the DRCWE was inserted into the liver parenchyma under ultrasonographic guidance (Figure 3a,b). The baseline power was set at 30 W. Ablation was continued with an increase of 10 W per minute until roll-off occurred. The power passively decreases to <10 W when tissue impedance rises above 200 Ω. Simultaneously, ^{18}F-fluorodeoxyglucose (^{18}F-FDG) was slowly injected into the liver by an automatic infusion syringe at a speed of 3 cm^3/min to evaluate the spread of ^{18}F-FDG by positron emission tomography (PET)/magnetic resonance imaging (MRI) examination (Figure 3c). After the RF energy was fully delivered for 10 min in the penetrated liver parenchyma, all electrodes were slowly removed when the electrode temperature reached approximately 70 °C to prevent tract bleeding along the tip. Three pigs were euthanized with a lethal injection of potassium chloride immediately after the procedure.

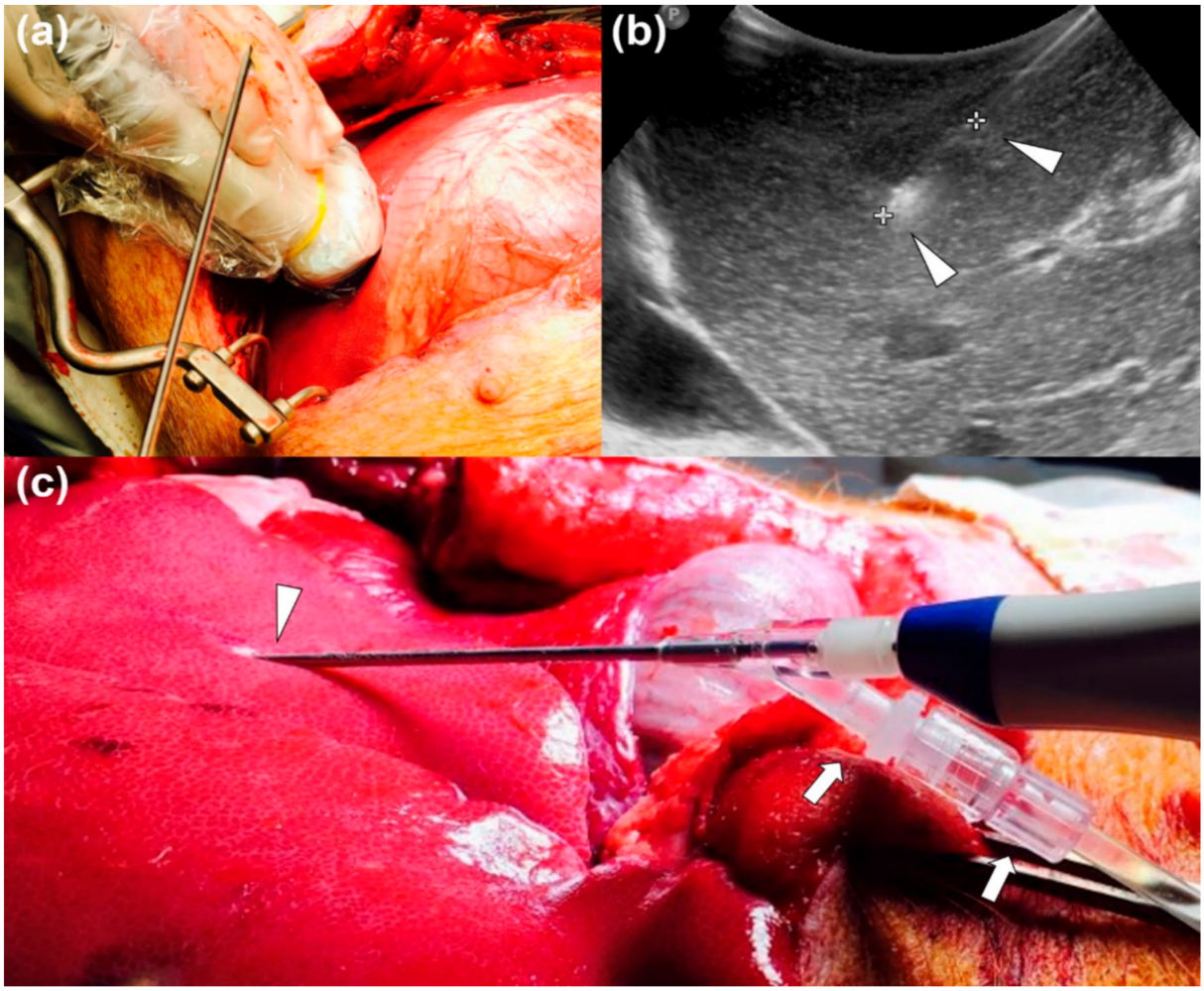

Figure 3. Radiofrequency ablation (RFA) procedural details. (**a**) Intraoperative view during the drug-releasing RFA in a pig under sonographic guidance. (**b**) The drug-releasing cooled wet electrode was inserted into the liver parenchyma. (**c**) ^{18}F-fluorodeoxyglucose was simultaneously slowly injected (arrow) during the RFA procedure.

2.3. Ex Vivo PET/MRI Examination

Surgical exploration of the liver was followed by the PET/MRI examination after sacrifice. The extracted liver was wrapped in a plastic wrap, which is a thin, transparent, plastic material to prevent drying out during image acquisitions by minimizing the occurrence of a motion artifact. The ablated portion was analyzed by the PET/MRI examination to investigate whether ^{18}F-FDG was exactly released and diffused. For this process, a commercial sequential nanoScan® PET/MRI system (Mediso Ltd., Hungary, Budapest) with ^{18}F-FDG was utilized to evaluate the drug that had been locally delivered on the

ablation zone. The total acquisition time for PET/MRI was 40 min. Moreover, MRI scans were performed immediately following the PET image acquisitions simultaneously in the same scanner. Total continuous images of PET (range, 170–200) and MRI (range, 350–350) were obtained from section slices, which have a thickness of 4 and 3 mm, respectively. After the PET images were reconstructed using the 3D row action maximum-likelihood algorithm with 3D spherically symmetric basis functions, the physiologic data were fused with MRI using the Syntegra software (version 2.1F; Philips, Eindhoven, The Netherlands), which can automatically superimpose physiologic data (PET) with anatomic data (MRI), eliminating the need for clinicians to manually identify and match the information.

2.4. Measurement of the Ablation Zone

The liver specimens were dissected along the axis of the electrode insertion and were sliced again in the plane perpendicular to the electrode tracks. The central white area was considered the zone of coagulative necrosis. The diameters of the maximum (D_{max}), minimum (D_{min}), and vertical diameter (D_v) of the central white area of the RFA zones were measured. The images of the ablation zones were analyzed using ImageJ software (version 1.53, National Institutes of Health, Bethesda, MD, USA). The dimensions were measured thrice by two observers, and the average dimensions were used to minimize the measurement error. To calculate the ablated volumes (AV), the following formulas were used:

$$\mathrm{AV} = \frac{\pi}{6}(D_{max} \times D_{min} \times D_v) \quad (1)$$

The circularity of the ablation zones was evaluated by the ratio between the D_{max} and D_{min}. Moreover, the retention rate was defined as the ratio of the ^{18}F-FDG radioactivity concentration derived from the PET/MRI images as follows: retention rate = (estimated dose/injection dose) × 100. Furthermore, to calculate the image volumes (IV) of ^{18}F-FDG uptake in the liver and measure the standard uptake value (SUV), the regions of interest were drawn manually and measured by one experienced nuclear medicine physician. The SUV was calculated as follows:

$$\mathrm{SUV} = \frac{(\text{Tissue Concentration (MBq/mL)})}{\left(\frac{\text{Injected Dose (MBq)}}{\text{Body Weight (g)}}\right)} \quad (2)$$

2.5. Statistical Analysis

The results of continuous variables were expressed as the mean ± standard deviation (SD). The differences between the AV and IV were compared using the Mann–Whitney U test (nonparametric method). All p values were two-sided. Moreover, a value <0.05 was considered statistically significant. Statistical analysis was performed using the SPSS software (version 24.0; IBM, Chicago, IL, USA).

3. Results

3.1. Procedural Outcomes

All three pigs tolerated the RFA procedures under laparotomy, with no major changes in their vital signs on the electrocardiography during the procedure. Moreover, drug-releasing RFA was technically successful without procedural-related complications. The color changes of the ablated zones of the liver were observed in all specimens during the procedure (Figure 4). The intraoperative ultrasonography also showed typical echogenic clouds in the RFA-created ablation zones of the liver.

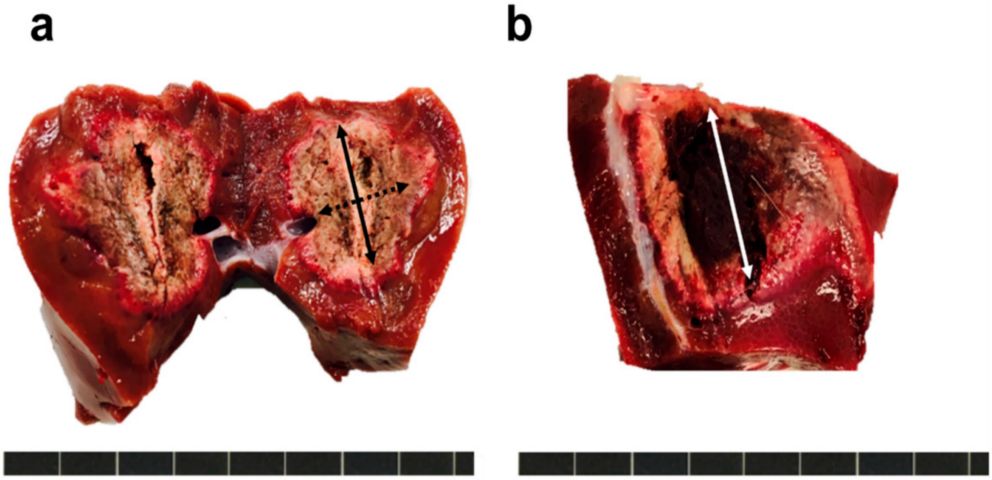

Figure 4. The elliptical shape of a radiofrequency ablation (RFA) zone created by the drug-releasing cooled wet electrode. (**a**) A specimen in the electrode insertion axis. D_{max} and D_{min} indicate maximum diameter (black solid arrow) and minimum diameter (black dotted arrow). (**b**) A specimen in the transverse plane perpendicular to the electrode insertion axis. D_v indicates vertical axis (white solid arrow).

3.2. Analysis of Ablation Zone of the Liver

The mean of the total delivered power according to the ablation duration (per minute) was 1.04 kcal/min. All measurement values of the ablation zone are shown in Table 1. The mean values of D_{max}, D_{min}, and D_v were 3.56 ± 0.19, 2.56 ± 0.27, and 3.12 ± 0.09 cm, respectively. In addition, the AV in the porcine liver and circularity was 15.22 ± 2.30 cm^3 and 0.72 ± 0.08, respectively.

The IV and ^{18}F-FDG measurement values are shown in Table 1. The mean IV around the ablated lesion was 17.21 ± 2.85 cm^3 (Figure 5). This was higher than the AV (17.21 ± 2.85 vs. 15.22 ± 2.30 cm^3) in the nine ablated lesions. Additionally, a statistically significant difference exists between the AV and IV (p = 0.008). The mean ^{18}F-FDG injection dose and the mean-estimated dose from PET/MR images were 7.13 ± 0.84 mCi/30 mL and 5.19 ± 0.60 mCi/30 mL, respectively. The retention rate ranged between 66.35% and 76.97%, and the mean retention rate percentage was 79.89% ± 4.22%. Also, the mean SUV showed 0.44 ± 0.05 (range, 0.375–0.541; Table 1).

Table 1. All measured values of the ablated porcine liver with use of a drug-releasing RFA system.

	D_{min} (cm)	D_{max} (cm)	D_v (cm)	AV (cm^3)	IV (cm^3)	Circularity	Injection Dose (mCi/30 mL)	Estimated Dose (mCi/30 mL)	Retention Rate (%)	SUV
1.1	2.32	3.24	3.1	12.20	14.12	0.72	6.94	5.02	72.33	0.458
1.2	2.46	3.74	3.14	15.19	17.21	0.66	7.45	5.70	76.51	0.541
1.3	2.22	3.51	3.04	12.40	14.31	0.63	5.46	3.86	70.70	0.484
2.1	3.01	3.41	3.17	17.03	18.91	0.88	7.03	5.27	74.96	0.375
2.2	2.93	3.88	3.21	19.10	22.67	0.76	6.47	4.98	76.97	0.398
2.3	2.48	3.6	3.01	14.06	15.79	0.69	7.10	5.46	76.90	0.465
3.1	2.41	3.64	3.29	15.10	19.10	0.66	7.81	5.84	74.78	0.431
3.2	2.67	3.49	3.02	17.43	18.30	0.77	7.43	4.93	66.35	0.396
3.3	2.5	3.52	3.14	14.47	14.50	0.71	8.45	5.62	66.51	0.405
Mean (± SD)	2.56 ± 0.27	3.56 ± 0.19	3.12 ± 0.09	15.22 ± 2.30	17.21 ± 2.85	0.72 ± 0.08	7.13 ± 0.84	5.19 ± 0.60	72.89 ± 4.22	0.44 ± 0.05

Data are shown as means ± standard deviation (SD). D_{min}, minimum diameter of the ablation zone; D_{max}, maximum diameter of the ablation zone; D_v, vertical diameter of the ablation zone; AV, the ablated volumes; IV, the image volume measured on PET-MR; circularity, the ratio between the D_{max} and D_{min}; retention rate = (estimated dose/injection dose) × 100, SUV, standard uptake value; there was significant difference between AV and IV ($p = 0.008$).

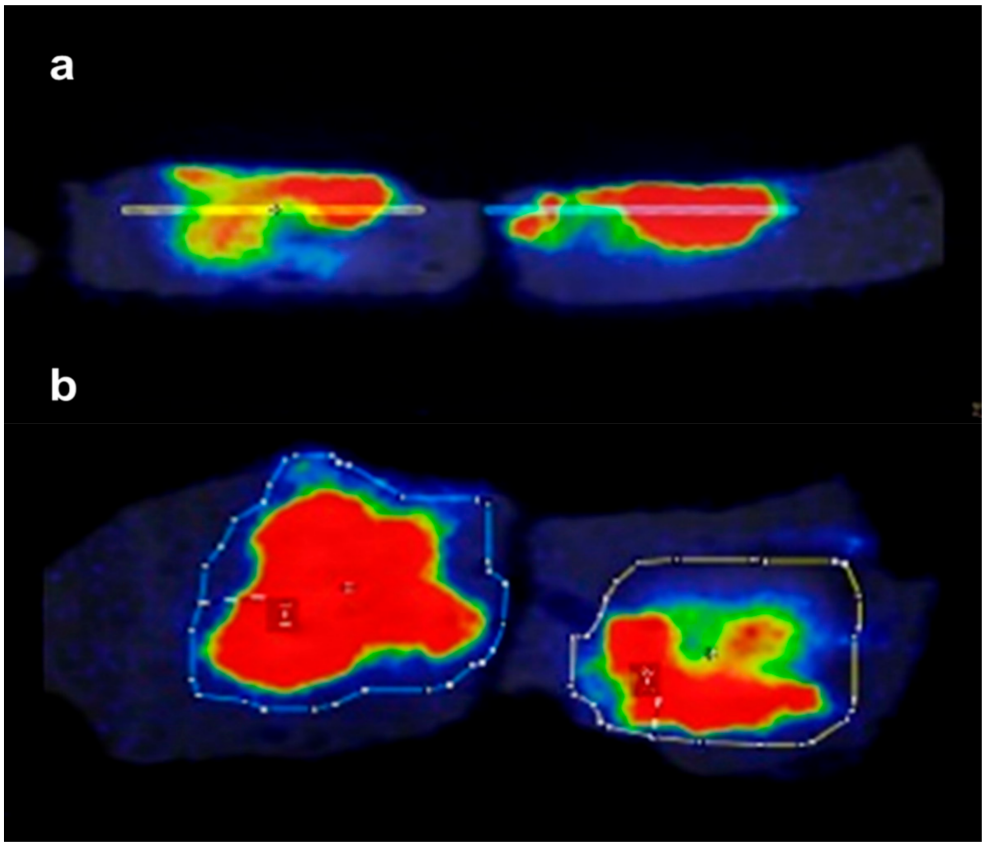

Figure 5. ^{18}F-fluorodeoxyglucose (^{18}F-FDG)-positron emission tomography/magnetic resonance imaging examination imaging in the extracted liver. (**a**) Sagittal sections of the extracted liver. (**b**) The focal ^{18}F-FDG uptake on transverse cut sections was calculated by drawing the regions of interest.

4. Discussion

This study using DRCWE was able to perform ablations and successfully delivered the drug in the ablation zone margin. The results of the experiment demonstrated that the coagulation zone using DRCWE could be created with the mean diameter (D_{max}, 3.56 ± 0.19; D_{min}, 2.56 ± 0.27) and AV of 15.22 ± 2.30 cm^3, which seems to be within the range of those of other studies [18,19]. Furthermore, circularity > 0.70 could indicate that the ablated lesions were circular. Additionally, the IV was considerably higher than the AV (17.21 ± 2.85 vs. 15.22 ± 2.30 cm^3) with statistically significant differences. This suggested that the released drug could effectively prevent local recurrence around the ablated lesions. In addition, the SUV as a simple image-based measure, which is widely used in clinical practice, was used to remove variability introduced by differences in animal size and the amount of injected FDG [20,21]. The mean SUV was 0.44 ± 0.05, which means that 40% of the drug has been released to the surroundings. Thus, adjusting the amount of the drug to take this into account would be better.

Considering that creating at least a 5-mm safety zone around the tumor is necessary to decrease local recurrence after RFA for primary and secondary liver malignancies, the results of this study indicate that DRCWE can successfully treat a 3.5-cm-diameter tumor without creating an overlapping ablation. Therefore, DRCWE may not only be a successful treatment for HCC but may also lower the recurrence rate by releasing the anticancer drug to residual cancer cells after RFA.

FDG-PET sensitivity for detecting HCC is approximately 50–70% [22]. Although the exact sensitivity was unknown because the normal liver model was used in this experiment, a similar retention rate was measured, which was 72.89% ± 4.22% (range, 66.35–76.97%). Here, high retention rates of >70% on average may be seen as evidence that the DRCWE RFA system can be useful.

Local tumor recurrence is defined as the reappearance of enhancing tissue within and around the ablation zone, which is secondary to the presence of residual viable or unablated tumor in patients previously considered to have complete ablation. The reported local recurrence rates after RFA ranged from 2% to 60% and have been currently managed by hepatic resection, salvage liver transplantation, and repeated RFA [23,24]. However, retreatment for local recurrence is often difficult and has a high failure risk [25,26]. A recent impact study reported the use of chemotherapy and bevacizumab with or without RFA for the treatment of unresectable liver metastases in patients with colorectal cancer [27]. Therefore, it is believed that DRCWE may reduce the local tumor recurrence rate after RFA by utilizing the chemotherapeutic agents in patients with HCC and may also increase the RFA indications to include larger liver malignancies.

A tendency to leave viable tumor cells in the margins or clefts of overlapping ablation zones for large tumors was noted (i.e., >3 cm diameter) although RFA is more effective for small-sized tumors (i.e., <3 cm diameter) [28–30]. Therefore, the ablation of larger liver tumors increases the possibility of incomplete ablation or local recurrence. The local failure rate of these tumors was high at the site of the primary tumor as well as elsewhere within the liver at sites remote from the treatment location due to vascular spread [30]. In this situation, multiple overlapping treatments with either a single electrode or multiple electrodes to increase the ablation zone size were utilized as the common method to resolve this RFA problem [31]. However, the precise repositioning of an electrode as a contiguous method and the accurate positioning of multiple electrodes can still be technically challenging [32]. Therefore, we believe that DRCWE may help to increase clinical outcomes with a relatively low recurrence rate after RFA by delivering anti-cancer drug, and it may also expand the RFA indications for large tumors.

Limitations and Future Direction

Several technical considerations were noted in the application of this method for the direct treatment of large livers, despite RFA with DRCWE resulting in a good outcome. First, further investigation with more animals and liver cancer models is needed to exactly evaluate the efficacy. Second, the gross examination of specimens was performed for the size measurement of ablation zones instead of histological analysis. The grossly measured size of the ablation zones may not be perfectly equal to the size of the actual coagulated tissue although gross appearance correlates with histological findings. In fact, because our results were simply represented the pharmacological response to therapeutic intervention (drug + RFA) by measuring the zone of coagulative necrosis, it was difficult to accurately evaluate the drug released extent. Third, the varying dimensions were measured thrice for each specimen and represented the mean value ± SD. However, the possibility of an assessment error exists due to manual measurements. Fourth, we did not evaluate RFA only or drug-releasing only treated the porcine liver as a control group because of a limited number of animals. A comparative study is required for accurate evaluation. Further improvement in reproducibility to increase the efficiency of anticancer drug delivery to the ablation zone should be warranted. Nevertheless, this study could provide a reliable basis for testing the DRCWE feasibility.

5. Conclusions

The drug-releasing RFA system was feasible not only for local ablations but also for the delivery of anticancer drugs. The results of this study indicate that this localized RFA with a drug delivery system could be a promising option for the prevention of local recurrence rates after RFA.

Author Contributions: Conceptualization, K.W.K. and J.-H.P.; Methodology, K.W.K. and Y.C.C.; Investigation, Y.C.C., S.J.H., J.H.J. and K.W.K.; Formal Analysis, S.J.H. and J.H.J.; Data Curation, K.B.L.; Validation. Y.C.C.; Writing—Original Draft Preparation, Y.C.C. and K.B.L.; Writing—Review & Editing, K.B.L., K.W.K. and J.-H.P.; Visualization, Y.P. and D.-S.W.; Supervision, K.W.K.; Funding Acquisition, J.-H.P. All authors have read and agreed to the published version of the manuscript.

Funding: This work was supported by the Korea Medical Device Development Fund grant funded by the Korea government (the Ministry of Science and ICT, the Ministry of Trade, Industry and Energy, the Ministry of Health & Welfare, the Ministry of Food and Drug Safety) (Project Number: KMDF_PR_20200901_0079) and by the National Research Foundation of Korea (NRF) grant funded by the Korea government (MSIT) (2021R1A2B5B03001891). MSIT: Ministry of Science and ICT.

Institutional Review Board Statement: This study was approved by the Institutional Animal Care and Use Committee of the Asan Institute for Life Sciences (2016-13-005) and conformed to US National Institutes of Health guidelines for humane handling of laboratory animals.

Informed Consent Statement: Not applicable.

Data Availability Statement: The data presented in this study are available on request from the corresponding author. The data are not publicly available due to ethical issues.

Conflicts of Interest: The authors declare no conflict of interest.

References

1. Wah, T.M.; Arellano, R.S.; Gervais, D.A.; Saltalamacchia, C.A.; Martino, J.; Halpern, E.F.; Michael, M.; Mueller, P.R. Image-guided percutaneous radiofrequency ablation and incidence of post–radiofrequency ablation syndrome: Prospective survey. *Radiology* **2005**, *237*, 1097–1102. [CrossRef] [PubMed]
2. Choi, J.W.; Lee, J.M.; Lee, D.H.; Yoon, J.-H.; Kim, Y.J.; Lee, J.-H.; Yu, S.J.; Cho, E.J. Radiofrequency ablation using internally cooled wet electrodes in bipolar mode for the treatment of recurrent hepatocellular carcinoma after locoregional treatment: A randomized prospective comparative study. *PLoS ONE* **2020**, *15*, e0239733. [CrossRef] [PubMed]
3. Curley, S.A.; Izzo, F.; Delrio, P.; Ellis, L.M.; Granchi, J.; Vallone, P.; Fiore, F.; Pignata, S.; Daniele, B.; Cremona, F. Radiofrequency ablation of unresectable primary and metastatic hepatic malignancies: Results in 123 patients. *Ann. Surg.* **1999**, *230*, 1–8. [CrossRef] [PubMed]
4. Decadt, B.; Siriwardena, A.K. Radiofrequency ablation of liver tumours: Systematic review. *Lancet Oncol.* **2004**, *5*, 550–560. [CrossRef]
5. Shiina, S.; Tateishi, R.; Arano, T.; Uchino, K.; Enooku, K.; Nakagawa, H.; Asaoka, Y.; Sato, T.; Masuzaki, R.; Kondo, Y.; et al. Radiofrequency ablation for hepatocellular carcinoma: 10-year outcome and prognostic factors. *Am. J. Gastroenterol.* **2012**, *107*, 569–577. [CrossRef]
6. McGhana, J.P.; Dodd, G.D. Radiofrequency Ablation of the Liver Current Status. *Am. J. Roentgenol.* **2001**, *176*, 3–16. [CrossRef] [PubMed]
7. Shiina, S.; Teratani, T.; Obi, S.; Sato, S.; Tateishi, R.; Fujishima, T.; Ishikawa, T.; Koike, Y.; Yoshida, H.; Kawabe, T.; et al. A randomized controlled trial of radiofrequency ablation with ethanol injection for small hepatocellular carcinoma. *Gastroenterology* **2005**, *129*, 122–130. [CrossRef]
8. Lin, S.M.; Lin, C.J.; Lin, C.C.; Hsu, C.W.; Chen, Y.C. Radiofrequency ablation improves prognosis compared with ethanol injection for hepatocellular carcinoma <or =4 cm. *Gastroenterology* **2004**, *127*, 1714–1723.
9. Lencioni, R.A.; Allgaier, H.P.; Cioni, D.; Olschewski, M.; Deibert, P.; Crocetti, L.; Frings, H.; Laubenberger, J.; Zuber, I.; Blum, H.E.; et al. Small hepatocellular carcinoma in cirrhosis: Randomized comparison of radio-frequency thermal ablation versus percutaneous ethanol injection. *Radiology* **2003**, *228*, 235–240. [CrossRef]
10. Machi, J.; Uchida, S.; Sumida, K.; Limm, W.M.; Hundahl, S.A.; Oishi, A.J.; Furumoto, N.L.; Oishi, R.H. Ultrasound guided radiofrequency thermal ablation of liver tumors: Percutaneous, laparoscopic, and open surgical approaches. *J. Gastrointest. Surg.* **2001**, *5*, 477–489. [CrossRef]
11. Goldberg, S.N.; Gazelle, G.S.; Solbiati, L.; Rittman, W.J.; Mueller, P.R. Radiofrequency tissue ablation: Increased lesion diameter with a perfusion electrode. *Acad. Radiol.* **1996**, *3*, 636–644. [CrossRef]
12. Rossi, S.; Buscarini, E.; Garbagnati, F.; Stasi, M.D.; Quaretti, P.; Rago, M.; Zangrandi, A.; Andreola, S.; Silverman, D.; Buscarini, L. Percutaneous treatment of small hepatic tumors by an expandable RF needle electrode. *Am. J. Roentgenol.* **1998**, *170*, 1015–1022. [CrossRef] [PubMed]
13. Miao, Y.; Ni, Y.; Yu, J.; Zhang, H.; Baert, A.; Marchal, G. An ex vivo study on radiofrequency tissue ablation: Increased lesion size by using an "expandable-wet" electrode. *Eur. Radiol.* **2001**, *11*, 1841–1847. [CrossRef]
14. Goldberg, S.N.; Solbiati, L.; Hahn, P.F.; Cosman, E.; Conrad, J.E.; Fogle, R.; Gazelle, G.S. Large-volume tissue ablation with radio frequency by using a clustered, internally cooled electrode technique: Laboratory and clinical experience in liver metastases. *Radiology* **1998**, *209*, 371–379. [CrossRef]
15. Lee, J.M.; Han, J.K.; Lee, J.Y.; Kim, S.H.; Choi, J.Y.; Lee, M.W.; Choi, S.H.; Eo, H.; Choi, B.I. Hepatic radiofrequency ablation using multiple probes: Ex vivo and in vivo comparative studies of monopolar versus multipolar modes. *Korean J. Radiol.* **2006**, *7*, 106–117. [CrossRef]
16. Lee, J.M.; Han, J.K.; Kim, H.C.; Choi, Y.H.; Kim, S.H.; Choi, J.Y.; Choi, B.I. Switching monopolar radiofrequency ablation technique using multiple, internally cooled electrodes and a multichannel generator: Ex vivo and in vivo pilot study. *Investig. Radiol.* **2007**, *42*, 163–171. [CrossRef]

17. Lee, J.M.; Han, J.K.; Chang, J.M.; Chung, S.Y.; Kim, S.H.; Lee, J.Y.; Lee, M.W.; Choi, B.I. Radiofrequency ablation of the porcine liver in vivo: Increased coagulation with an internally cooled perfusion electrode. *Acad. Radiol.* **2006**, *13*, 343–352. [CrossRef] [PubMed]
18. Yu, M.H.; Lee, J.Y.; Jun, S.R.; Kim, K.W.; Kim, S.H.; Han, J.K.; Choi, B.I. Radiofrequency Ablation with an Internally Cooled Monopolar Directional Electrode: Ex Vivo and in Vivo Experimental Studies in the Liver. *Radiology* **2016**, *278*, 395–404. [CrossRef] [PubMed]
19. Brace, C.L.; Sampson, L.A.; Hinshaw, J.L.; Sandhu, N.; Lee, F.T. Radiofrequency ablation: Simultaneous application of multiple electrodes via switching creates larger, more confluent ablations than sequential application in a large animal model. *J. Vasc. Interv. Radiol.* **2009**, *20*, 118–124. [CrossRef]
20. Kinahan, P.E.; Fletcher, J.W. PET/CT Standardized Uptake Values (SUVs) in Clinical Practice and Assessing Response to Therapy. *Semin. Ultrasound CT MR* **2010**, *31*, 496–505. [CrossRef] [PubMed]
21. Brendle, C.; Kupferschläger, J.; Nikolaou, K.; Fougère, C.L.; Gatidis, S.; Pfannenberg, C. Is the standard uptake value (SUV) appropriate for quantification in clinical PET imaging?—Variability induced by different SUV measurements and varying reconstruction methods. *Eur. J. Radiol.* **2015**, *84*, 158–162. [CrossRef]
22. Cho, K.J.; Choi, N.K.; Shin, M.H.; Chong, A.R. Clinical usefulness of FDG-PET in patients with hepatocellular carcinoma undergoing surgical resection. *Ann. Hepatobiliary Pancreat. Surg.* **2017**, *21*, 194–198. [CrossRef]
23. Chan, A.C.Y.; Chan, S.C.; Chok, K.S.H.; Cheung, T.T.; Chiu, D.W.; Poon, R.T.P.; Fan, S.T.; Lo, C.M. Treatment strategy for recurrent hepatocellular carcinoma: Salvage transplantation, repeated resection, or radiofrequency ablation? *Liver Transpl.* **2013**, *19*, 411–419. [CrossRef]
24. Muaddi, H.; Al-Adra, D.P.; Beecroft, R.; Ghanekar, A.; Moulton, C.-A.; Doyle, A.; Selzner, M.; Wei, A.; McGilvray, I.D.; Gallinger, S.; et al. Liver Transplantation is Equally Effective as a Salvage Therapy for Patients with Hepatocellular Carcinoma Recurrence Following Radiofrequency Ablation or Liver Resection with Curative Intent. *Ann. Surg. Oncol.* **2018**, *25*, 991–999. [CrossRef]
25. Mulier, S.; Ni, Y.; Jamart, J.; Ruers, T.; Marchal, G.; Michel, L. Local Recurrence After Hepatic Radiofrequency Coagulation: Multivariate Meta-Analysis and Review of Contributing Factors. *Ann. Surg.* **2005**, *242*, 158–171. [CrossRef]
26. Poon, R.T.P.; Fan, S.T.; Wong, J. Risk Factors, Prevention, and Management of Postoperative Recurrence After Resection of Hepatocellular Carcinoma. *Ann. Surg.* **2000**, *232*, 10–24. [CrossRef] [PubMed]
27. Yasuno, M.; Uetake, H.; Ishiguro, M.; Mizunuma, N.; Komori, T.; Miyata, G.; Shiomi, A.; Kagimura, T.; Sugihara, K. mFOLFOX6 plus bevacizumab to treat liver-only metastases of colorectal cancer that are unsuitable for upfront resection (TRICC0808): A multicenter phase II trial comprising the final analysis for survival. *Int. J. Clin. Oncol.* **2019**, *24*, 516–525. [CrossRef] [PubMed]
28. Livraghi, T.; Goldberg, S.N.; Lazzaroni, S.; Meloni, F.; Ierace, T.; Solbiati, L.; Gazelle, G.S. Hepatocellular carcinoma: Radiofrequency ablation of medium and large lesions. *Radiology* **2000**, *214*, 761–768. [CrossRef] [PubMed]
29. Park, M.J.; Kim, Y.S.; Rhim, H.; Lim, H.K.; Lee, M.W.; Choi, D. A comparison of US-guided percutaneous radiofrequency ablation of medium-sized hepatocellular carcinoma with a cluster electrode or a single electrode with a multiple overlapping ablation technique. *J. Vasc. Interv. Radiol.* **2011**, *22*, 771–779. [CrossRef]
30. Goldberg, S.N.; Gazelle, G.S.; Mueller, P.R. Thermal ablation therapy for focal malignancy: A unified approach to underlying principles, techniques, and diagnostic imaging guidance. *Am. J. Roentgenol.* **2000**, *174*, 323–331. [CrossRef] [PubMed]
31. Beiderwellen, K.; Gomez, B.; Buchbender, C.; Hartung, V.; Poeppel, T.D.; Nensa, F.; Kuehl, H.; Bockisch, A.; Lauenstein, T.C. Depiction and characterization of liver lesions in whole body 18F-FDG PET/MRI. *Eur. J. Radiol.* **2013**, *82*, e669–e675. [CrossRef] [PubMed]
32. Beiderwellen, K.; Geraldo, L.; Ruhlmann, V.; Heusch, P.; Gomez, B.; Nensa, F.; Umutlu, L.; Lauenstein, T.C. Accuracy of 18F-FDG PET/MRI for the Detection of Liver Metastases. *PLoS ONE* **2015**, *10*, e0137285. [CrossRef] [PubMed]